

The Thermal Performance of Reflective Insulation Materials and Systems with Horizontal Heat Flow: A Parametric Study

A.O. Desjarlais

R.P. Tye

ABSTRACT

An experimental program involving a total of approximately 100 guarded hot box (ASTM 1987) experiments has been developed and performed on well-characterized test panels containing reflective insulation materials and typical products. The test panels contained additional internal temperature instrumentation to obtain the necessary data to determine the thermal performance of the reflective insulation material from the test results on the systems. The experimental matrix included tests to measure the effect of airspace mean temperature and temperature difference, cavity emittance and aspect ratio, heat flow direction, and the interaction between multiple airspaces within a single cavity. This paper reports only the horizontal heat flow experiments portion of the program.

The experimental results for 48 guarded hot box tests on a series of reflective insulation systems are presented, together with two different one-dimensional calculations used to determine the thermal resistance of the reflective airspace: an isothermal planes method and a parallel path technique. The parallel path calculation procedure used in this program has been proposed in the draft ASTM Standard Specification for "Reflective Insulation for Building Applications." A comparison to the work which forms the basis of the thermal performance of airspaces detailed in the ASHRAE Handbook of Fundamentals (ASHRAE 1989) is also included and discussed.

The results from this program indicate that the thermal resistance of test panels containing reflective airspaces increases disproportionately with the number of airspaces, increases with decreasing temperature difference, and did not exhibit a significant mean temperature effect. Data that are presently used to predict the thermal performance of reflective airspaces overstate that performance for multiple airspace cavities. The proposed method for determining the cavity thermal resistance from test panel experiments has also been verified.

INTRODUCTION

A comprehensive assessment was undertaken for the Department of Energy (Yarbrough 1983) on the subject of reflective insulations. This assessment discussed the controversial issues relating to the thermal performance of these systems. These issues included questions regarding applicability of current data on air spaces bounded by reflective surfaces (Robinson and Powelitch 1956; Bejan 1980; ASHRAE 1985), appropriate test methods, specimen configurations and analytical models used to derive results (Hollingsworth 1983, 1987; Poppendiek 1983; ASHRAE 1985; Miller et al. 1987), and the resultant disparities in thermal performance data.

A.O. Desjarlais, Manager, Thermal Insulation Evaluation and R.P. Tye, Business Development Manager, Holometrix, Inc.

Some recommendations were made in the assessment on how these issues could be resolved. The major short-term recommendation was to undertake a comprehensive experimental laboratory study supported by well-validated heat transfer models. As a result, an investigation designed to satisfy the stated objectives was developed and initiated under the Department of Energy (DOE) Building Thermal Envelope Systems and Materials (BTESM) program. This investigation has been described in detail (Desjarlais and Tye 1989).

One important feature of this program was the establishment of a review panel consisting of individuals, including ASHRAE members, from industry, government, and academia. Each member of the panel had some relevant experience in the subject of reflective insulations. The purpose of this panel was to monitor the progress of the program and advise the investigators. Thus, all industry sectors were included in this coordinated approach. The involvement of the DOE was beneficial to the reflective insulation community and also fulfilled a number of objectives in the current National Program Plan (BTECC 1988).

The technical approach was to develop an acceptable test and evaluation protocol, generate an initial data base on some idealized systems, and extend this data base to a limited number of commercial product types such that adequate analytical models to predict thermal performance could be developed and verified. A corollary to this program was the verification of the calculational procedure for determining the thermal performance of reflective insulation, which has been proposed in the ASTM Standard Specification for "Reflective Insulation for Building Applications."

The present paper contains the results and analysis for the horizontal heat flow experimentation only, extracted from a portion of a larger test program designed to address questions regarding reflective insulation thermal performance. The overall program involved the generation and analysis of an extremely large volume of data for approximately 50 systems/test conditions for each of the vertical and horizontal heat flow orientations. This division into two approximately equal phases allows the results to be presented conveniently for the horizontal and vertical heat flow directions separately.

TEST MATRIX AND DETAILS OF THE TEST PANELS

Table 1 contains details of the 48 experiments performed on 10 different configurations during this program.

A schematic of a typical test panel is shown in Figure 1. The test panels were constructed with 2 by 4 studs placed 16 in. on center forming a panel with an overall cross section of 96 in. by 96 in. The test panels were constructed such that the center of the test panel aligned with the center of the central cavity. For the guarded hot box used in this program, three full cavities were in the metered area. A 1/4-in.-thick plywood material was used to sheath both sides of the test panel. The plywood is an atypical sheathing but was selected to minimize the additional thermal resistance that the sheathing added to the test panel.

Panels 1A, 1B, 3A, 3B, 3C, and 4A were constructed with extruded polystyrene foam (XEPS) studs. These studs were fabricated by slicing 3 1/2-in.-wide strips from a nominal 1 1/2-in.-thick board and installing them in the test panel such that the predominant heat flow direction in the stud would be along the extruded polystyrene foam board. Panels 2A, 2B, 2C, and 4B were constructed with kiln-dried wood studs. The plywood sheathing was attached to the wood studs with 1 1/4-in.-drywall screws located 12 in. on center. To attach the sheathing to the XEPS studs, 1/4-in.-diameter nylon-threaded rods were installed into holes drilled through the sheathings and XEPS studs. These holes were situated 16 in. on center; there were 8 nylon rods in the metering area. The sheathing was held in place by tightening nylon nuts onto each side of the threaded rods.

To create a single reflective airspace having an effective emittance, E , of approximately 0.05, a single sheet of an aluminum foil paper laminate reflective insulation material, supplied by a reflective insulation manufacturer, was adhered to the interior side of the hot-side sheathing material. An 1/8-in.-wide thermal break was cut into the reflective insulation around the perimeter of the metering area. A single cavity having an effective emittance of 0.03 was constructed by applying the reflective insulation material to the interior sides of both sheathings. Two airspace cavities, with each airspace having an effective emittance of 0.03, were fabricated by installing a sheet of reflective insulation material in the center of the cavity thickness and laminating both sheathings with the reflective insulation material. To hold the central foil in place, the width of the reflective insulation material installed in the center of the cavity was adjusted so that the material could be folded and attached directly to the stud. The width of the attachment flange was 1 in. In the wood stud test panel, the flanges were stapled to the stud. Staples were applied 12 in. on center. To hold the central foil to the XEPS studs, the flanges were pressed against the stud with a 1-by 1/2-in. fiberglass angle and held in place with 1/8-in.-diameter threaded nylon rods and nuts spaced 12 in. on center. The four airspace cavities were created by utilizing a commercial three-layer product supplied by a reflective insulation manufacturer. The thickness of each airspace in this cavity was approximately 7/8 in. The application of this product followed the manufacturer's instructions. Attachment to the wood and XEPS studs was identical to the methods used on the central foils of the two airspace cavity systems.

Tests were also performed on a test panel, with each type of stud material, insulated with a nominal R-11 fiberglass batt insulation. These experiments were performed to verify that the subsequent calculations could accurately deduce the thermal resistance of the cavity insulation from the system R-Value test.

THERMAL RESISTANCE AND EMITTANCE OF TEST PANEL COMPONENTS

The thermal resistance of the two stud materials, the plywood sheathing, and the fiberglass batt insulation material was tested in accordance with ASTM C 518-85 (ASTM 1987). Samples of the stud materials approximately 24 in. square in cross section by 3 1/2-in.-thick were prepared by gluing sixteen 1 1/2-in.-wide by 24-in.-long sections of stud material. This sample preparation technique allowed for the testing of the studs in the same orientation to their use in the test panel. A 24-in.-square sample of the fiberglass insulation material was prepared by sandwiching two 5-in.-wide by 24-in.-long sections of material around a full width (14 1/2-in.) by 24-in.-long section. These samples were analyzed utilizing a large heat flow meter apparatus which has been previously described (Tye et al. 1987). A 12-in.-square sample of the sheathing was prepared and tested in a small heat flow meter apparatus. This instrument has also been previously described (Howard et al. 1973).

The emittance of the single layer and each surface of the three-foil multilayer reflective insulation material along with samples of the wood and XEPS studs, wood sheathing, and foil and duct tapes that were used to attach the temperature instrumentation to the various surfaces of the test panel were measured using an emissometer. Multiple (at least 10) measurements were performed on each material (Yarbrough and Cook 1988).

The thermal resistance and emittance results of these test panel components are presented in Tables 2 and 3, respectively. The thermal resistance of the stud materials, sheathing, and fiberglass batt are within 9% of data listed for these products in the ASHRAE Handbook of Fundamentals (ASHRAE 1985). The emittance of the XEPS is lower than originally expected. Difficulties in experimentally determining the emittance of a thick thermally resistive sample may account for this result.

TEST PANEL INSTRUMENTATION AND THERMAL RESISTANCE TESTING

The thermal resistance of the test panels was measured in accordance with ASTM C 236-87 (ASTM 1987). The test facility used to perform these analyses has previously been described (Tye et al. 1981; Tye and Desjarlais 1987). Through participation in one round-robin series of measurements on polyisocyanurate foam board products, the precision of the hot boxes has been shown to be better than 5% (Sherman 1981). More recently, through involvement in the ASTM C-16/NBS hot box round-robin, the precision of this hot box was shown to be better than 2% when compared to the group mean (Bales 1985). The laboratory is also accredited by the Department of Commerce through the National Voluntary Laboratory Accreditation Program (NVLAP) for performing tests in accordance with ASTM C 236.

The test facility has a metering area of 48.5 in. square located in the center of the 96-in.-square test panel. For this series of experiments, the air velocity parallel to the hot and cold surfaces of the test panels was 0.6 and 1.0 ft/sec, respectively.

Convective breaks or stops fabricated from 1 1/2-in.-thick XEPS were used along the top and bottom portions of the metering box perimeter to prevent air exchange between the metering and guard areas of the test panel. Convective stops were also installed in the adjoining guard area cavities in an attempt to replicate the convective loops of the metering area.

In addition to the instrumentation routinely used when performing guarded hot box experiments, 34 thermocouples were installed to measure the temperature of critical locations inside the test panel. A set of thermocouples was installed in an area-weighted array on each major vertical surface (inside each sheathing, on central foil in two airspace cavities, and on each foil in four airspace cavities). Depending on the emittance of the instrumented surface, these thermocouples were attached and thermally grounded to the surface with either aluminum foil or duct tape. These sensors allowed for the measurement of the temperature difference across the cavity and each individual airspace within the cavity. Five thermocouples were installed in an "H" pattern into one of the central studs to measure the temperature of the interfaces between the stud and sheathings and therefore the temperature difference across the stud. Small grooves were cut into the faces of the studs to accommodate these sensors. Thermocouples were also installed on each side of the top and bottom convective breaks and the studs forming the vertical boundaries of the metering area to measure the temperature difference and therefore the energy exchange between the metering area and the surrounding cavities.

TEST RESULTS AND DISCUSSION

The measured total energy input (Q_{total}), heat flow through the stud (Q_{stud}), mean temperature and temperature difference test conditions (T_{mean} and ΔT), and panel surface-to-surface thermal resistance (R) for the experiments performed are summarized in the "Measured Panel" columns of Table 4. The procedure used to calculate Q_{stud} is described below. The guarded hot box used for these measurements has a metering box area of 16.34 ft².

The impact of the stud material on the thermal resistance of the test panels can be measured by comparing the results of test panels 4A and 4B. These test panels were constructed with XEPS and wood studs, respectively, and their cavities were filled with unfaced R-11 fiberglass batts. The same insulation batts were used in the metering area for both test panels. The measured panel thermal resistances of these two test panels were 12.21 and 9.75 h ft² °F/Btu at the same approximate test conditions.

Test panels 1A, 2A, and 3A were constructed as single airspace systems. The differences in the construction of these three test panels were the framing material (XEPS for test panels 1A and 3A, wood for test panel 2A) and the effective emittance of the airspace (0.05 for test panel 1A, 0.03 for

test panels 2A and 3A). Testing on test panel 1A was performed exclusively with an airspace mean temperature of 50°F. Testing on the other two panels was undertaken predominantly at an airspace mean temperature of 75°F with single analyses at 50°F. The panel thermal resistance test results gathered at the predominant airspace mean temperature were fitted as a function of temperature difference. These curve-fit coefficients are listed in Table 5. A comparison of the test results gathered on these panels shows the following:

1. The panel R-values for 1A (XEPS, $E = 0.05$, $T_{mean} = 50^\circ\text{F}$) and 2A (wood, $E = 0.03$, $T_{mean} = 75^\circ\text{F}$) agree to within ± 0.05 hr ft² °F/Btu. The increases in heat transfer due to the low thermal resistance wood stud and higher mean temperature of 2A are offset by the lower effective emittance of the airspace. Results on both test panels show an increasing panel thermal resistance as the airspace temperature difference decreases.

2. The panel R-values for 1A (XEPS, $E = 0.05$, $T_{mean} = 50^\circ\text{F}$) are 0.4 hr ft² °F/Btu lower than 3A (XEPS, $E = 0.03$, $T_{mean} = 75^\circ\text{F}$). This difference is primarily due to the difference in the effective emittance of the airspace. A comparison of tests H-29 and H-34 on 3A indicates no effect on the panel thermal resistance due to differences in cavity mean temperature. The latter conclusion is corroborated by comparing the results of tests H-11 and H-16 on test panel 2A.

3. The heat flow through the framing members, Q_{stud} , ranged from 1.6% to 2.4% of the metering box energy input for the XEPS studs and from 5.3% to 6.6% for the wood studs. The small percentages of Q_{stud} are due to the relatively low thermal resistances of the cavities or airspaces of these test panels.

4. To compare these test results to data gathered previously, it is necessary to adjust the results for the sheathing materials used. A composite stud/cavity thermal resistance can be computed by subtracting twice the sheathing thermal resistance found in Table 2 from the test panel result. A similar exercise employed on other data sets will yield comparable results.

A similar analysis can be performed on the two-airspace systems, test panels 1B, 2B, and 3B. Similar to the single-airspace systems, the differences in the construction of these three test panels were the framing material (XEPS for test panels 1B and 3B, wood for test panel 2B) and the effective emittance of the airspace (0.05 for test panel 1B, 0.03 for test panels 2B and 3B). Testing on test panel 1B was performed such that the mean temperature of the airspace on the cold side of the cavity was 50°F while the hot side airspace mean temperature varied from 60° to 100°F. Testing conditions on the other two panels were designed such that the hot-side airspace mean temperature was predominantly 75°F with single analyses at 50°F while the cold-side airspace mean temperature varied from 35° to 70°F. Since testing conditions on panel 1B are different than those imposed on panels 2B and 3B, direct comparisons cannot be made. However, the following observations are noted.

1. Results on all three test panels show an increasing panel thermal resistance as the airspace temperature difference decreases.

2. The panel R-values for 1B (XEPS, $E = 0.05$, $T_{mean} = 56^\circ$ to 73°F) and 2B (wood, $E = 0.03$, $T_{mean} = 56^\circ$ to 73°F) agree to within ± 0.08 h ft² °F/Btu. Similar to the one-airspace systems, the increases in heat transfer due to the low thermal resistance wood stud of 2B are offset by the lower effective emittance of the airspace.

3. The panel R-values for 1B (XEPS, $E = 0.05$, $T_{mean} = 56^\circ$ to 73°F) are 0.8 h ft² °F/Btu lower than 3B (XEPS, $E = 0.03$, $T_{mean} = 57^\circ$ to 75°F). This difference is due to the effective emittance of the airspace and is twice the difference noted for the same comparison on single-airspace systems.

4. The heat flow through the framing members, Q_{stud} , ranged from 2.6% to 5.0% of the metering box energy input for the XEPS studs and from 7.7% to 13.6% for the wood studs. As the thermal resistance of the airspace increases, a larger percentage of the metering box energy input is transferred through the studs.

5. Comparisons with other panel test results can be performed by adjusting the results for the sheathing materials used. The procedure described for the one-airspace cavities would again be employed. The panel thermal resistance test results for the two-airspace systems were fitted as a function of cavity temperature difference and the curve-fit coefficients are listed in Table 5.

A comparison of the panel thermal resistance test results of the four-airspace systems, test panels 3B and 3C, indicates similar behavior. The only difference in the construction of these two panels was the framing material (XEPS for test panel 3C, wood for test panel 2C). The panels were subjected to identical test conditions. The panel thermal resistance test results for the four-airspace systems were fitted as a function of cavity temperature difference and the curve-fit coefficients are listed in Table 5. The following observations are noted.

1. Results on the two four-airspace test panels show an increasing panel thermal resistance as the airspace temperature difference decreases.

2. The panel R-values for 3C (XEPS) exceed 2C (wood) by approximately 0.9 h ft² °F/Btu.

3. The heat flow through the framing members, Q_{stud} , ranged from 3.8% to 5.0% of the metering box energy input for the XEPS studs and from 10.2% to 12.8% for the wood studs.

4. The thermal resistance of panel 3B (two airspaces with XEPS studs) exceeds the thermal resistance of panel 2C (four airspaces with wood studs).

Table 4 also includes the results obtained for the cavity thermal resistance calculated by two different methods, $R_{(||)}$ and $R_{(ISO)}$, the cavity mean temperature and temperature difference (T_{mean} and dT), and a prediction of the cavity thermal resistance based on the original work of Robinson and Powelitch (1956), $R_{(predicted\ cavity)}$.

Two different one-dimensional calculations were used to separate the thermal performance of the reflective insulation material from the test panel thermal performance: the parallel path method, $R_{(||)}$, and the isothermal planes method, $R_{(ISO)}$ (ASHRAE 1985). The parallel path method is identical to the procedure that is presently recommended for inclusion into the proposed ASTM Standard Specification for reflective insulations. The following equations were used to perform these calculations:

$$Q_{total} = Q_{stud} + Q_{cavity} \quad (1)$$

$$R_{(||)} = (dT_{cav}) * A_{cav} / (Q_{total} - Q_{stud}) \quad (2)$$

$$R_{(ISO)} = A_{cav} / (A_{total} / (R_{total} - R_{sheath}) - A_{stud} / R_{stud}) \quad (3)$$

where

Q_{total} = total metering box energy input

Q_{stud} = heat flow through studs calculated with the temperature measurements of the T/Cs in the studs and the R-values of the studs measured by ASTM C 518

Q_{cavity} = the heat flow through the cavity determined by correcting the total metering box energy input by the stud heat flow

dTcav = ΔT as measured by T/Cs mounted on the interior of the sheathing

Acav = the metering area of the panel that is cavity

Atotal = the total metering area of the panel

Rtotal = the measured surface-to-surface R-value of the panel including the sheathing

Rsheath = the measured R-value of the sheathing by ASTM C 518

Astud = the metering area of the panel that is stud

Rstud = the measured R-value of the stud by ASTM C 518.

A prediction of the cavity thermal resistance was performed utilizing the curve-fitting coefficients developed by Yarbrough when he applied the method of least squares to the data generated by Robinson and Powelitch (Yarbrough 1983). The use of these coefficients allowed for the prediction of the cavity thermal resistance for the exact temperature conditions of the experiment. When there was more than a single airspace forming the cavity, the thermal resistance of each individual airspace was determined and summed. The temperature sensors installed in the test panels allowed for the direct measurement of the temperature difference across each airspace.

The predicted cavity thermal resistance and the percent difference between the prediction and the calculated cavity thermal resistance for each calculation procedure are shown in Table 4 and the differences as a function of number of airspaces are summarized in Figure 2. The following equation was used to determine the percent differences:

$$\% \text{ Difference} = \left(\frac{R_{\text{predicted}} - R_{\text{calculated}}}{R_{\text{predicted}}} \right) \quad (4)$$

Both calculation methods agreed extremely well with the predicted thermal resistance for single airspaces: 0.5% for the parallel path method and -0.2% for the isothermal planes method. The predicted thermal performance of the two- and four-airspace cavities were significantly higher than either calculation method for determining the cavity thermal resistance. Average differences of 19.1% and 18.1% for the two-airspace cavities and 62.2% and 62.2% for the four-airspace cavities were noted for the parallel path and isothermal planes models, respectively. Both calculation techniques agreed extremely well. An average difference of only 0.7% was noted between the calculated cavity thermal resistances determined by the two techniques.

The cavity thermal resistance calculated by the parallel path method for all the test panels using wood and XEPS stud framing members is shown graphically as a function of cavity temperature difference in Figures 3 and 4, respectively. Significant increases in cavity R-value are noted as the temperature difference across the cavity decreases for all the test panels studied. A 13% and 17% increase was noted in the thermal resistance of the one- and two-airspace cavities when the effective cavity emittance was decreased from 0.05 to 0.03. The R-value of the two-airspace cavities exhibited a greater increase, due probably to the enhanced effect of the radiative component of heat transfer due to the smaller airspace temperature differences per airspace. The idealized two-airspace cavity performed almost as well as the four-airspace cavity created by a commercial product. This result suggests that significant improvements can be obtained with the commercial product through a redesign of the flange which maintains the foil spacing and holds the product in place.

The Series 2 test panels (2A, 2B, and 2C) were different than the respective Series 3 test panels (3A, 3B, and 3C) only in the material used for the stud or framing material. The Series 2 and 3 test panels used wood and XEPS studs, respectively. The average difference between the predicted

cavity and calculated cavity thermal resistances as a function of stud type and number of airspaces within the cavity is shown graphically in Figure 5. The average difference between the cavity thermal resistance test results calculated by the parallel path method and the predicted performance for the wood and XEPS stud framing members was 28.4% and 23.4%, respectively. As the number of airspaces forming the cavity increases, the heat flow through the stud becomes a larger percentage of the total heat flow and any errors due to uncertainties in the stud thermal resistance should be magnified. For any particular configuration, the heat flow correction due to the framing members is significantly smaller for the XEPS studs due to its higher thermal resistance. The inability to note any significant improvement in the prediction of the cavity thermal resistance due to a reduction in the stud heat flow by substituting a high-resistance material for the stud suggests that accurate information regarding the thermal resistance of the framing material was obtained. If this information is unavailable, reducing the stud heat flow by material substitution would reduce the importance of this lack of knowledge.

To test the effect of cavity temperature difference on the accuracy of the measurement of the cavity thermal resistance, all of the differences between the calculated cavity and the predicted R-value data for one-airspace cavities were plotted as a function of cavity temperature difference and are shown in Figure 6. This analysis was limited to the one-airspace systems because dissimilar cavity temperature differences were used for the test panels. For cavity temperature differences of 20°F or more, the ability to measure the temperature difference does not appear to impact the quality of the measurement. A temperature difference of 20°F or more should be used when analyzing these products.

The proposed ASTM Standard Specification requires that the heat flow correction for the framing members be corroborated by repeating the experiment with the test panel cavities filled with a mass insulation. A representative sample of the mass insulation would be previously tested and the predicted thermal resistance of the mass insulation must agree with its directly measured thermal resistance to within 10%. To check the stringency of this requirement, two test panels (4A and 4B) were insulated with unfaced R-11 fiberglass batts and tested. The same insulation batts were used in the metering area for both test panels. The average density of these batts was 0.61 lb/ft³. To determine the cavity thermal resistance, the fiberglass batt that had been originally tested at a thickness of 3.5 in. and a density of 0.74 lb/ft³ was expanded to obtain the same density as the product in the metering area. The retesting of the fiberglass blanket at the same density as the metering area material was used as the predicted cavity thermal resistance. The predicted cavity thermal resistance differed with the calculated cavity thermal resistance by -1.7% and +7.5% for the XEPS and wood stud test panels, respectively.

Due to the presence of convective loops within the airspaces, convective blocks were installed at the perimeter of the metering area to prevent any air exchange between the metered and guard areas. Sections of 1 1/2-in.-thick XEPS foam were used along the top and bottom of the perimeter while framing members (wood or XEPS) aligned with the vertical perimeter of the metered area. To determine the energy exchange between the metered and guard areas, temperature sensors were installed on the convective blocks and framing members that formed the exterior boundary of the metering area. Temperature differences of up to 69°F (test number H-17) were noted across the horizontal convective blocks but these differences were always coupled with an approximately equivalent temperature difference across the opposing block. The largest mismatch between the temperature differences across the top and bottom convective blocks was 14.9°F (test number H-35), yielding an additional metering area energy input of 2 Btu/h for an experiment having a metering area energy input of 367 Btu/h. The average mismatch between the temperature differences across the top and bottom convective blocks was approximately 4.5°F. The vertical members of the metering/guard area boundary had much smaller temperature differences across them, averaging approximately 1.1°F. For wood studs, the average energy exchange was less than 1.5 Btu/h.

CONCLUSIONS

Based on this test program, the following conclusions have been drawn.

1. The thermal resistance of all the test panels increases with decreasing cavity temperature differences. Reductions in temperature difference reduce the convective heat transfer across the airspace.

2. The data that are presently used in the ASHRAE Handbook of Fundamentals as a basis for determining the thermal resistance of airspaces agree with the measurements performed only when the cavity is comprised of a single airspace. As the number of airspaces increases, the data increasingly overpredict the cavity thermal resistance. Differences of 1%, 19%, and 62% were noted for one-, two-, and four-airspace cavities, respectively.

3. The two calculation techniques used to determine the cavity thermal resistance of the test panels work equally well. Similar results were obtained by both methods.

4. Decreasing the cavity emittance from 0.05 to 0.03 yielded increases in the cavity thermal resistance of 13% and 17% for one- and two-airspace cavities, respectively.

5. The idealized two-airspace and the commercial four-airspace cavities have approximately the same thermal resistance, suggesting significant improvements in the performance of commercial products could be obtained.

6. The average cavity thermal resistance of all of the experiments performed with wood and XEPS framing members differed by approximately 5%, with the XEPS test panels predicting the higher cavity thermal resistance.

7. The experimental data suggest that cavity temperature differences of at least 20°F are required to perform accurate measurements.

8. The proposed ASTM test panel verification process was tested. The density of the entire metering area should be measured and a test sample of similar density should be used for determining the target cavity thermal resistance.

9. Temperature instrumentation around the perimeter of the metering area was used to measure any energy exchange between the metering and guard areas. Although large temperature differences resulting from convective loops were measured, net energy exchange was very small when compared to the metering box energy input.

REFERENCES

- ASHRAE. 1985. ASHRAE handbook of fundamentals, Chapter 23. Atlanta: American Society of Heating, Refrigerating, and Air-Conditioning Engineers, Inc.
- ASTM. 1985. ASTM C 518-85, Standard Test Method for "Steady-state heat flux measurements and thermal transmission properties by means of the heat flow meter apparatus" ASTM Standards, Vol. 04.06, pp. 201-217. Philadelphia: American Society of Testing and Materials.
- ASTM. 1987. ASTM C 236-87, Standard Test Method for "Steady-state thermal performance of building assemblies by means of a guarded hot box" ASTM Standards, Vol. 04.06, pp. 63-77. Philadelphia: American Society of Testing and Materials.
- Bales, E.L. 1985. "ASTM/DOE hot box round robin" Proceedings of ASTM C16.30 Symposium, Colorado Springs, CO, March.
- Bejan, A. 1980. "A synthesis of analytical results for natural convection heat transfer across rectangular enclosures" Int. J. Heat Mass Transfer, Vol. 23, p. 723.

- Building Thermal Envelope Coordinating Council. 1988. "The national program plan for the thermal performance of building envelope systems and materials." Washington, DC.: Building Thermal Envelope Systems and Materials.
- Desjarlais, A.O., and Tye, R.P. 1989. "Evaluation of the thermal performance of reflective insulation materials and systems" ASHRAE Transactions, Vol. 95, Part 2.
- Hollingsworth, M.J., Jr. 1983. "Experimental determination of the thermal resistance of reflective insulations" ASHRAE Transactions, Vol. 2, 89, Part 1.
- Hollingsworth, M.J., Jr. 1987. "Thermal testing of reflective insulation." Thermal Insulation Materials and Systems, eds. F.J. Powell and S.M. Matthews. ASTM STP 922, pp. 506-517. Philadelphia: American Society of Testing and Materials.
- Howard, J.K.; Coumou, K.G.; and Tye, R.P. 1973. "Direct thermal conductivity instrument with digital read-out for measurement of heat transmission in cellular plastics." J. Cellular Plastics, Vol. 9, p. 226.
- Miller, R.G.; Oscar, D.S.; Seiface, F.; and Goss, W.P. 1987. "Methods for determining the thermal performance of reflective insulation systems." Presented at ASTM C16 Symposium on Thermal Insulation Materials and Systems, Bal Harbour, FL, 6-9 December.
- Poppendiek, J.R.; Connelly, D.J.; and Fowler, E.W. 1983. "Some remarks on heat transfer in installed foil insulation systems." ASHRAE Transactions, Vol. 89, Part 1.
- Robinson, H.E., and Powlitch, F.J., 1956. "The thermal insulating value of airspaces." Housing Research Paper 32, United States National Bureau of Standards, Project ME-12, sponsored by the Housing and Home Finance Agency, U.S. Government Printing Office.
- Sherman, M. 1981. "Aged thermal resistance (R-value) of foil-faced polyisocyanurate foam thermal insulation board." Thermal Performance of Exterior Envelopes of Buildings I, E.L. Bales, ed., ASHRAE SP28, pp. 952-964.
- Tye, R.P., and Desjarlais, A.O. 1987. "Aging characteristics of cellular plastic insulation materials and insulated building components." Polyurethane World Congress 1987: 50 Years of Polyurethanes, Frankfurt, FRG, Fachverband Schaumkunststoffe eV, pp. 91-98, New York: The Society of the Plastics Industry.
- Tye, R.P.; Desjarlais, A.O.; Spinney, S.C.; and Bourne, J.G. 1981. "Effective thermal performance of an insulated standard stud wall containing air gaps." Thermal Performance of Exterior Envelopes of Buildings I, E.L. Bales, ed., ASHRAE SP28, pp. 965-977.
- Tye, R.P.; Coumou, K.G.; Desjarlais, A.O.; and Haines, D.M. 1987. "Historical development of large heat flow meter apparatus for measurements of thermal resistance of insulations." In: Thermal Insulation: Materials and Systems, ASTM STP 922, F.J. Powell and S.L. Matthews, Eds., American Society for Testing and Materials. pp. 651-664. Philadelphia: American Society of Testing and Materials.
- Yarbrough, D.W. 1983. "Assessment of reflective insulations for residential and commercial applications." ORNL/TM-8891, October.
- Yarbrough, D.W., and Cook, J. 1988. Emittance measurements report.

TABLE 1

SUMMARY DESCRIPTION OF TEST PANELS AND CONDITIONS FOR
THE GUARDED HOT BOX STUDY

PANEL NO.	NO. OF TESTS	NO. OF AIRSPACES	E	FRAME MATERIAL	ASPECT RATIO	DELTA T/ AIRSPACE	AIRSPACE T mean
1A	5	1	0.05	XEPS	14	10-50F	50F
1B	5	2	0.05	XEPS	28	10-50F	50F
2A	6	1	0.03	WOOD	14	10-50F	50,75F
2B	6	2	0.03	WOOD	28	5-50F	35-100F
2C	6	4	0.05	WOOD	56	2.5-12.5F	30-95F
3A	6	1	0.03	XEPS	14	10-50F	50,75F
3B	6	2	0.03	XEPS	28	5-50F	35-100F
3C	6	4	0.05	XEPS	56	2.5-12.5F	30-95F
4A	1	1	0.82	XEPS	N/A	50F	75F
4B	1	1	0.82	WOOD	N/A	50F	75F

- Notes: 1. E is the effective emittance of each airspace in the cavity and is calculated by $E = 1 / [1/e_1 + 1/e_2 - 1]$ where e_1 and e_2 are the emittances of the surfaces bounding the airspace.
2. The aspect ratio of the airspace is defined as the ratio of airspace height and airspace thickness.
3. The cavities of Test Panels 4A and 4B are filled with fiberglass batts.

TABLE 2

THE APPARENT THERMAL CONDUCTIVITY AND THERMAL RESISTANCE
OF FOUR SPECIMENS OF BUILDING MATERIALS USED TO CONSTRUCT TEST PANELS

Specimen	Test Thickness	Density	Mean Temperature	Apparent Thermal Conductivity	Thermal Resistance
	inches	lbs/ft ³	F	Btu-in/hr ft ² F	hr ft ² F/Btu
XEPS Stud	3.50	1.95	76.9	0.214	16.35
Wood Stud	3.53	27.2	76.9	0.754	4.67
Sheathing	0.24	31.4	81.9	0.752	0.32
Fiberglass Batt	3.50	0.737	75.1	0.293	11.93
	4.25	0.607	75.2	0.318	13.36

TABLE 3

THE EMITTANCE OF NINE SPECIMENS OF BUILDING
MATERIALS USED TO CONSTRUCT TEST PANELS

Specimen	No. of Samples	Total No. of Tests	Emittance
XEPS Stud	2	N/A	0.51
Wood Stud	2	N/A	0.77
Sheathing	2	N/A	0.77
Single Layer Foil	7	61	0.052
Foil Tape	2	8	0.029
Duct Tape	1	4	0.70
Multilayer Outer Foil	3	12	0.027
Multilayer Inner Foil	3	15	0.029
Multilayer Inner Paper	3	15	0.85

Table 4

The Measured Panel and Calculated Cavity Thermal Resistances
and a Comparison to the Predicted Cavity Thermal Resistance

Test Panel	Test Number	Stud Material	Thermal Resistance, hr ft ² F/Btu @ F										X Difference, Pred. Vs. Calc.		
			Q Total	Q Stud	Measured Panel			Calculated Cavity				Predicted Cavity			
			Btu/hr	Btu/hr	R	Tmean	dT	R ()	R (ISO)	Tmean	dT	R	R ()	R (ISO)	
1A	H-1	XEPS	340.7	5.43	3.06	50.7	63.9	2.17	2.21	50.0	49.7	2.27	4.4	2.8	
	H-2	XEPS	265.0	4.92	3.16	50.7	51.3	2.27	2.30	50.1	40.3	2.36	3.8	2.6	
	H-3	XEPS	189.0	3.62	3.27	50.4	37.8	2.37	2.40	49.8	30.0	2.52	5.7	4.8	
	H-4	XEPS	117.3	2.44	3.57	51.2	25.6	2.63	2.67	50.8	20.6	2.78	5.4	3.7	
	H-5	XEPS	50.8	1.18	3.99	50.4	12.4	3.04	3.07	49.9	10.3	3.41	10.8	10.0	
1B	H-6	XEPS	426.7	11.30	4.26	72.8	111.4	3.26	3.33	70.7	92.5	4.25	23.3	21.8	
	H-7	XEPS	356.0	9.84	4.46	72.9	97.1	3.42	3.51	71.1	80.9	4.39	21.9	20.0	
	H-8	XEPS	244.4	7.21	4.76	66.3	71.2	3.70	3.79	64.6	59.9	4.82	23.2	21.2	
	H-9	XEPS	143.0	4.73	5.36	60.8	46.9	4.24	4.36	59.6	40.0	5.53	23.4	21.2	
	H-10	XEPS	60.2	2.34	6.27	55.5	23.1	5.14	5.23	54.7	20.3	6.92	25.8	24.4	
2A	H-11	WOOD	330.9	17.62	3.11	76.3	63.0	2.37	2.34	74.3	50.7	2.31	-2.6	-1.4	
	H-12	WOOD	251.9	13.97	3.22	75.2	49.6	2.48	2.45	73.7	40.3	2.42	-2.7	-1.3	
	H-13	WOOD	191.0	10.80	3.32	74.9	38.8	2.57	2.55	73.2	31.6	2.55	-0.7	-0.1	
	H-14	WOOD	111.7	6.72	3.54	75.3	24.2	2.81	2.78	74.0	20.1	2.89	3.0	3.9	
	H-15	WOOD	51.5	3.41	3.91	75.7	12.3	3.23	3.16	74.2	10.6	3.53	8.5	10.7	
	H-16	WOOD	333.1	17.51	3.11	52.0	63.4	2.34	2.34	50.0	50.4	2.39	1.9	1.9	
2B	H-17	WOOD	416.2	31.94	4.28	73.0	109.1	3.52	3.55	71.9	92.2	4.50	21.8	21.0	
	H-18	WOOD	350.6	27.48	4.37	56.3	93.7	3.60	3.64	55.0	79.3	4.77	24.6	23.7	
	H-19	WOOD	236.7	20.25	4.77	60.7	69.1	4.02	4.07	59.8	59.4	5.17	22.2	21.1	
	H-20	WOOD	137.5	13.34	5.38	66.5	45.3	4.69	4.75	65.9	39.7	5.89	20.4	19.3	
	H-21	WOOD	56.9	6.65	6.46	70.6	22.5	5.92	5.99	70.1	20.3	7.36	19.5	18.5	
	H-22	WOOD	23.7	3.20	7.52	73.8	10.9	7.15	7.27	73.2	10.0	8.83	19.0	17.7	
2C	H-23	WOOD	154.2	15.68	5.71	74.5	53.9	5.27	5.12	73.6	49.8	14.60	63.9	64.9	
	H-24	WOOD	116.0	12.34	5.97	75.6	42.4	5.57	5.42	74.7	39.4	15.30	63.6	64.6	
	H-25	WOOD	81.7	9.24	6.44	75.9	32.2	6.04	5.96	75.1	29.9	16.07	62.4	62.9	
	H-26	WOOD	55.2	6.44	6.63	76.2	22.4	6.31	6.19	75.3	21.0	16.90	62.6	63.4	
	H-27	WOOD	22.7	2.91	7.41	74.6	10.3	7.18	7.13	73.7	9.7	18.21	60.6	60.8	
	H-28	WOOD	149.6	16.29	6.13	52.7	56.1	5.54	5.60	51.4	50.4	15.06	63.2	62.8	
3A	H-29	XEPS	292.3	5.52	3.41	76.4	61.0	2.47	2.53	75.4	48.4	2.33	-6.2	-8.6	
	H-30	XEPS	230.7	4.48	3.54	77.5	50.0	2.60	2.65	76.6	40.1	2.41	-7.7	-9.9	
	H-31	XEPS	153.7	3.20	3.78	76.6	35.6	2.80	2.88	75.6	28.8	2.60	-7.7	-10.5	
	H-32	XEPS	95.3	2.11	4.01	76.0	23.4	3.05	3.09	75.0	19.4	2.92	-4.5	-5.8	
	H-33	XEPS	49.5	1.20	4.42	75.8	13.4	3.40	3.47	74.8	11.2	3.47	1.9	-0.1	
	H-34	XEPS	292.8	5.64	3.42	50.9	61.3	2.51	2.54	50.1	49.1	2.40	-4.5	-5.8	
3B	H-35	XEPS	367.1	10.46	4.96	74.5	111.4	3.96	3.98	73.0	96.4	4.44	10.9	10.4	
	H-36	XEPS	299.4	8.70	5.05	56.7	92.6	4.04	4.07	55.2	80.1	4.75	15.1	14.4	
	H-37	XEPS	205.6	6.49	5.48	61.3	69.0	4.45	4.48	60.2	60.4	5.13	13.4	12.7	
	H-38	XEPS	119.2	4.25	6.19	66.0	45.2	5.12	5.16	65.2	40.2	5.87	12.7	12.0	
	H-39	XEPS	50.1	2.13	7.38	70.6	22.6	6.27	6.31	69.9	20.5	7.34	14.6	14.0	
	H-40	XEPS	21.1	1.06	8.66	73.1	11.2	7.60	7.58	72.5	10.4	8.77	13.3	13.5	
3C	H-41	XEPS	146.3	5.59	6.38	76.0	57.1	5.28	5.34	74.7	50.7	14.53	63.7	63.3	
	H-42	XEPS	109.0	4.31	6.67	76.9	44.5	5.57	5.62	75.7	39.8	15.26	63.5	63.2	
	H-43	XEPS	73.2	3.03	7.20	75.5	32.3	6.09	6.14	74.4	29.2	16.15	62.3	62.0	
	H-44	XEPS	44.9	2.12	8.04	75.9	22.1	6.92	6.97	74.8	20.2	16.99	59.3	59.0	
	H-45	XEPS	20.7	1.04	8.68	75.7	11.0	7.46	7.60	74.8	10.0	18.14	58.9	58.1	
	H-46	XEPS	133.4	5.54	6.95	51.6	56.8	5.66	5.90	49.9	49.4	15.20	62.8	61.2	
4A	H-47	XEPS	73.6	5.40	12.21	76.7	55.0	11.18	11.19	75.7	52.0	11.00	-1.7	-1.7	
4B	H-48	WOOD	83.6	15.03	9.75	74.9	49.9	10.17	10.22	74.0	47.6	11.00	7.5	7.1	

Table 5

The Fit Coefficients Used To Describe The Test Panel Thermal Resistance as a Function of Cavity Temperature Difference

Test Panel	Test Numbers	Fit Coefficients		
		A0	A1	A2
1A	H-1 TO H-5	4.531	-5.90E-02	5.98E-04
1B	H-6 TO H-10	7.399	-6.29E-02	3.18E-04
2A	H-11 TO H-15	4.327	-4.59E-02	4.38E-04
2B	H-17 TO H-22	8.278	-9.33E-02	5.49E-04
2C	H-23 TO H-27	8.026	-7.19E-02	5.14E-04
3A	H-29 TO H-33	4.966	-5.66E-02	5.12E-04
3B	H-35 TO H-40	9.515	-1.06E-01	6.16E-04
3C	H-41 TO H-45	9.744	-1.08E-01	8.16E-04

Note: $R = A_0 + A_1 \cdot dT + A_2 \cdot dT^2$ where:
 R = Test Panel Thermal Resistance, hr ft² F/Btu, and
 dT = Cavity Temperature Difference, F.

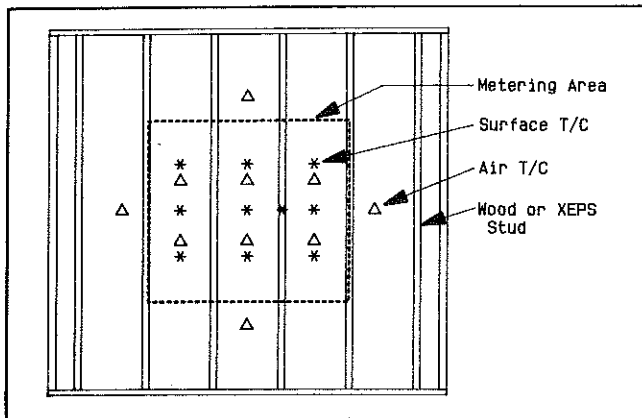


Figure 1. Schematic diagram of a typical test panel showing the metering area outline and the location of the temperature instrumentation

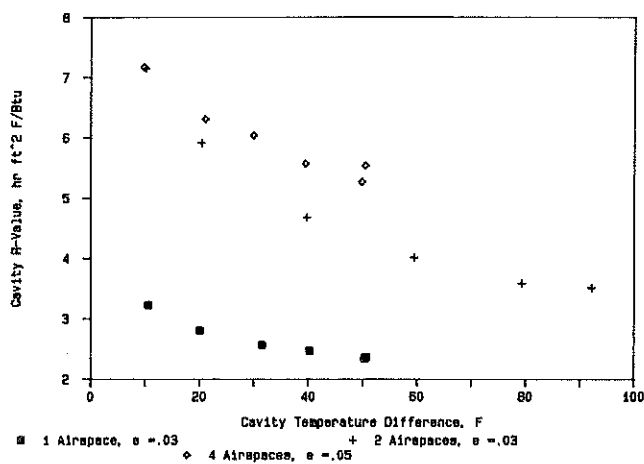


Figure 3. The calculated cavity thermal resistance of three airspaces as a function of cavity temperature difference from experiments on test panels with wood framing members

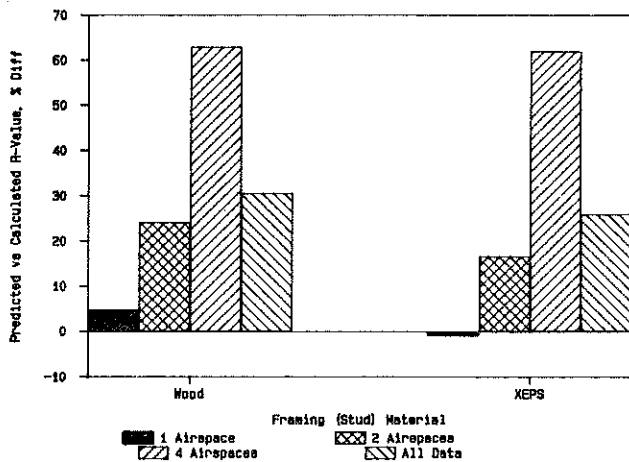


Figure 5. The percent difference between the predicted and calculated cavity thermal resistance as a function of framing material and the number of airspaces

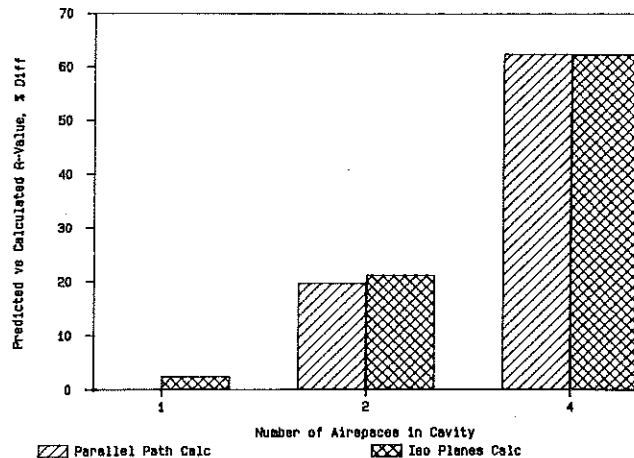


Figure 2. The percent difference between the predicted and calculated cavity thermal resistance as a function of the number of airspaces

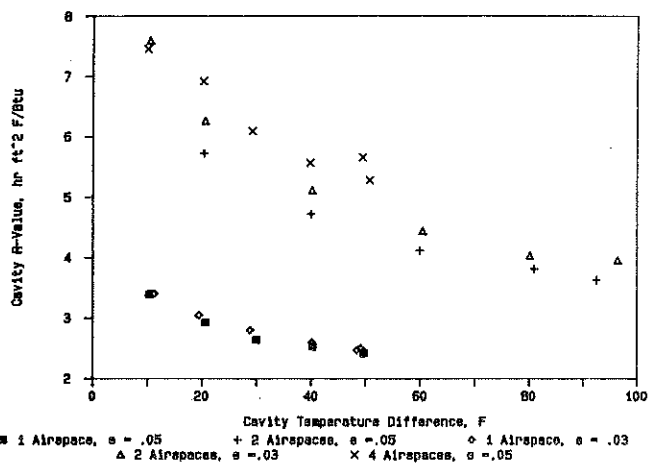


Figure 4. The calculated cavity thermal resistance of five airspaces as a function of cavity temperature difference from experiments on test panels with XEPS framing members

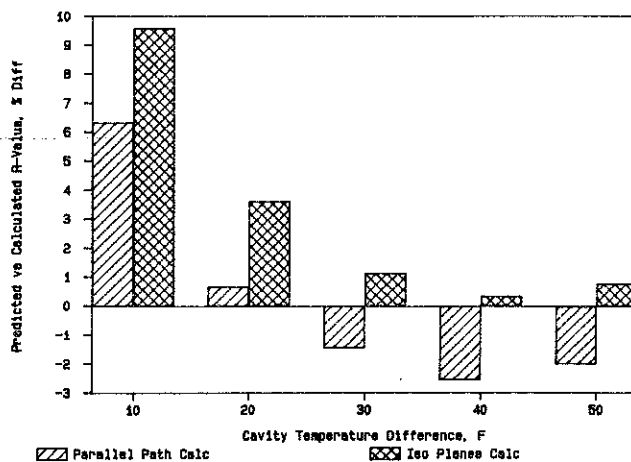


Figure 6. The percent difference between the predicted and calculated cavity thermal resistance of one-airspace cavities as a function of cavity temperature difference